Optical Amplification Using Raman Transitions between Spin-Singlet and Spin-Triplet States of a Pair of Coupled In-GaAs Quantum Dots

J. M. Elzerman, K. M. Weiss, J. Miguel-Sanchez, and A. Imamoğlu
Institute of Quantum Electronics, ETH Zurich, CH-8093 Zurich, Switzerland
(Received 6 December 2010; published 30 June 2011)

We report the observation of steady-state optical amplification in Raman transitions between the lowest-energy spin states of a single quantum-dot molecule. Absorption and resonance fluorescence experiments demonstrate that the entangled two-electron singlet and triplet states have electric-dipole coupling to a common optically excited state. Fast spin relaxation ensures optical gain on the triplet transition when the singlet transition is driven resonantly. By embedding the quantum-dot molecule in a cavity of modest quality factor, a solid-state single-emitter laser can be realized.

DOI: 10.1103/PhysRevLett.107.017401 PACS numbers: 78.67.Hc, 42.50.Ex, 78.30.Fs, 78.45.+h

A laser that uses a single quantum emitter as the gain medium [1] can exhibit a plethora of unusual features, including lasing without a well-defined threshold [2,3] and output intensity fluctuations that remain below the shot-noise limit [2,4,5]. For studies of these fundamental issues, single-atom lasers [6–8] with simple and well-understood level schemes have proven particularly suitable. On the other hand, compact devices capable of continuous-wave operation require monolithic structures involving a solid-state quantum emitter. Although signatures of lasing due to a single quantum dot (QD) in a nanocavity have been reported [9], the nature of the QD lasing states remains unclear, and most probably an intricate nonresonant cavity feeding mechanism is involved [10]. These complications have prevented a detailed understanding of the optical amplification process or the pumping mechanism in single QD lasers.

In this Letter, we report the observation of optical amplification [11,12] in a single coupled quantum-dot (CQD) molecule filled with two separate electrons. This novel solid-state quantum emitter combines an atomlike three-level lambda scheme, which can be fully characterized and driven coherently, with the tunability offered by solid-state technology. The optical amplification is a direct result of the interaction between the CQD and its solid-state environment, which induces fast relaxation between the spin-singlet and -triplet ground states.

The lambda scheme in this work is provided by a pair of vertically stacked self-assembled InGaAs QDs [13–17], separated by a thin GaAs tunnel barrier and embedded in a GaAs Schottky diode [Fig. 1(a)]. When both QDs contain a single electron—a charging regime denoted as $(1, 1)$—the lowest-energy levels correspond to spin-singlet (S) or -triplet (T_-, T_0, T_+) states [Fig. 1(b)]. Electron tunneling between the two dots gives rise to an exchange splitting between the $(1, 1)S$ and $(1, 1)T$ states [bottom panel in Fig. 1(c)], which allows us to selectively address them optically [16] even without a magnetic field. The size of the exchange splitting depends on the tunneling rate and can be tuned by varying the gate voltage [17].

The lowest-energy optical excitation corresponds to adding an electron-hole pair in the top dot (QD-R), which has a redshifted transition energy compared to the bottom dot (QD-B). The resulting fourfold degenerate excited states X [top panel in Fig. 1(c)] are labeled by the z component of the total angular momentum ($m_z = \pm 1, \pm 2$); this consists of a contribution from the heavy hole in QD-R ($m_z = \pm\frac{3}{2}$) plus the unpaired electron in QD-B ($m_z = \pm\frac{1}{2}$). From the associated optical selection rules [inset in Fig. 1(c)], it follows that states S and T_0 share two common optically excited states with $m_z = \pm 1$. At zero magnetic field, the selection rules are modified by the hyperfine interaction with the nuclear spins, which strongly mixes the three degenerate triplet states [18]. Likewise, the four degenerate optically excited states are mixed by both hyperfine interaction and indirect electron-hole exchange [17]. As a consequence, population in any X or T level is efficiently distributed among the entire X or T manifold, so that the full system can be represented by three levels (S, T, and X) in a simple lambda configuration, as illustrated in Fig. 4(b). In this Letter, we use this lambda system to achieve single-pass optical amplification of 0.014%. All measurements were performed at 4.2 K in a liquid-helium bath cryostat.

We first perform microphotoluminescence (PL), to select a CQD pair that exhibits the $(1, 1)$ charging regime. As the gate voltage is increased, the number of electrons in the CQD increases one by one. Therefore, the PL spectra in Fig. 2 show typical plateaus [19], separated by dotted vertical lines indicating a change in the ground state charge. Each plateau corresponds to emission from the neutral exciton or negatively charged trion in a particular dot. The detailed shape of the plateau for a given QD depends on the number of electrons in its partner dot, due to tunnel coupling [13–17] and charge sensing [20]. From these characteristic PL patterns we identify the CQD charging sequence as $(0, 0) \rightarrow (1, 0) \rightarrow (1, 1) \rightarrow (1, 2)$,

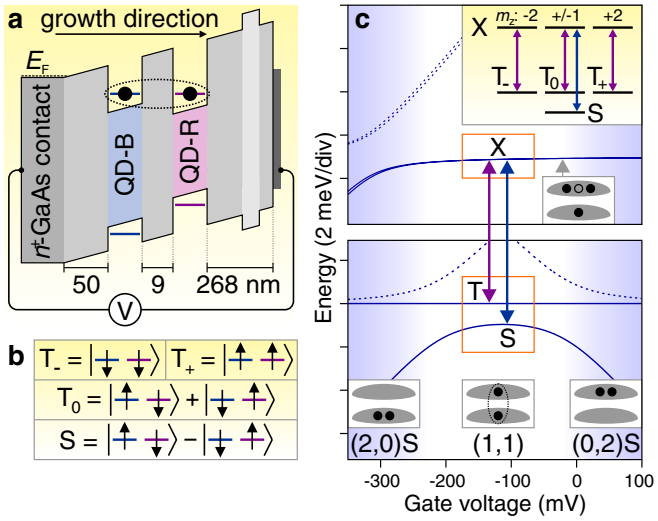

FIG. 1 (color online). (a) Schematic energy diagram of the device, containing two layers of self-assembled InGaAs QDs, separated by a 9 nm GaAs tunnel barrier and embedded in a GaAs Schottky diode. The voltage V applied between the Si-doped n^+-GaAs back contact and the semitransparent top gate (2 nm of Ti plus 8 nm of Au) controls the CQD charging state and allows both QDs of a pair to be filled with a single electron. (b) Spin-singlet (S) and -triplet (T) states in the $(1, 1)$ charging regime. (c) Energy diagram showing the different ground states (bottom panel) and optically excited states (top panel) versus V. State $(1, 1)S$ is coupled via electron tunneling to $(2, 0)S$ and $(0, 2)S$, in which both electrons reside in QD-B or QD-R, respectively (as illustrated in the gray boxes, where filled circles depict electrons and open circles holes). The coupling gives rise to two anticrossings between the S states that split $(1, 1)S$ from $(1, 1)T$, since the latter does not experience tunnel coupling to any of the S states [17]. Dashed lines indicate energy levels not used in the experiment. Inset: Optical selection rules for transitions from the $(1, 1)S$ and T states to the fourfold degenerate optically excited states X.

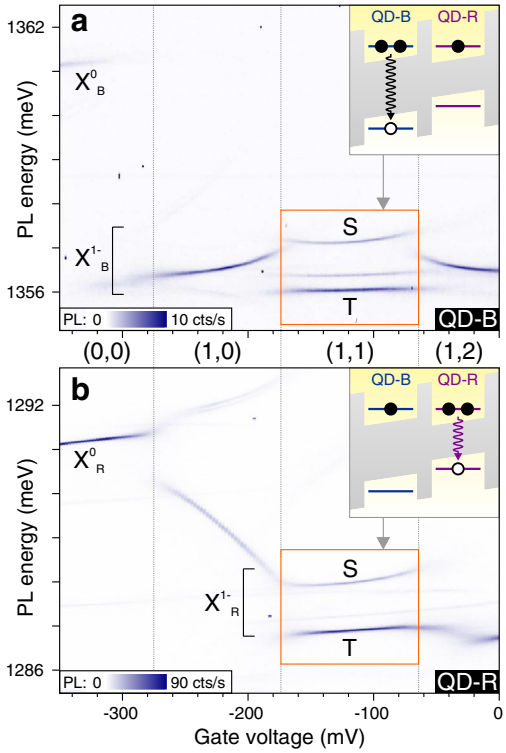

FIG. 2 (color online). PL (in color scale) as a function of gate voltage. (a) PL from QD-B. Dotted vertical lines separate regions with a different total number of electrons in the CQD; the inferred ground state charge distribution for each region is indicated below the panel. In the $(1, 1)$ charging region (highlighted by orange boxes), PL involving the S state is identified by its characteristic curvature and by its $\sim$3 times weaker intensity compared to PL involving the threefold degenerate T states. X^0_B (X^{1-}_B) indicates emission from the neutral exciton (negative trion) in QD-B. Inset: Schematic energy diagram illustrating X^{1-}_B emission in the $(1, 1)$ regime. Because holes can tunnel from QD-B to QD-R before recombination, PL from QD-B is weaker than that from QD-R. (b) PL from QD-R. X^0_R (X^{1-}_R) indicates emission from the neutral exciton (negative trion) in QD-R. Inset: Schematic energy diagram illustrating emission from the optically excited states X to states S or T in the $(1, 1)$ regime.

confirmed by using numerical simulations [21]. In the $(1, 1)$ regime, we find a 1.1 meV exchange splitting between the S and T states.

To establish the optical connection between the S and T states, we employ resonance fluorescence measurements [22]. When resonantly driving the S transition in QD-R [orange arrow in the upper trace of Fig. 3(a)], fluorescence is detected not only at the same energy (Rayleigh scattering) but also at an energy corresponding to the T transition (coherent and incoherent Raman scattering). Conversely, when driving the T transition in QD-R (orange arrow in the lower trace), additional weaker emission is observed at the S transition. These measurements demonstrate that the $(1, 1)S$ and T states indeed share common optically excited states X in which a negative trion is located in QD-R. Moreover, the fact that the T peak in the upper trace is $\sim$3 times stronger than the S peak implies that the fourfold degenerate states X are strongly mixed; without mixing, driving the S transition would only excite the $m_z = \pm 1$ subspace, resulting in an equal number of photons emitted on the T and S transitions [see the inset in Fig. 1(c)]. Together, these observations provide experimental justification for treating the system of one S, three T, and four X states as a simple lambda system, as illustrated in Fig. 4(b).

It is important to notice that driving the T transition results in much less fluorescence than driving the S transition, although both traces in Fig. 3(a) were taken with identical laser power. We find an S:T fluorescence ratio of $\sim$8 (taking into account the imperfect cancellation of the excitation laser). This asymmetry is also seen in differential transmission (dT) measurements throughout the $(1, 1)$ charging regime. On the S-X transition [Fig. 3(b)], scattering of resonant laser photons gives a dT contrast of -0.07%. The dT contrast of the T-X transition [Fig. 3(c)] is only -0.011%, i.e., $\sim$6 times smaller. This difference points towards the presence of effective spin relaxation

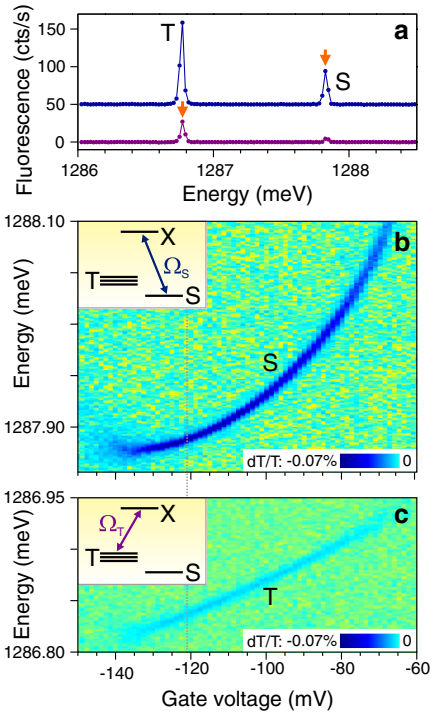

FIG. 3 (color online). (a) Resonance fluorescence detected with a spectrometer, when resonantly driving the S-X transition (upper trace) or the T-X transition (lower trace) close to saturation (Rabi frequencies $\Omega_{S,T} \sim 1$ μeV), at $V = -121$ mV. Orange arrows indicate the excitation energy. The reflected linearly polarized excitation laser is suppressed by using a polarizer. Traces are offset vertically for clarity. (b) Differential transmission dT/T (in color scale) of a laser (with $\Omega_S = 0.5$ μeV) scanned across the S-X transition versus V throughout the (1, 1) regime. Inset: Schematic energy diagram of the lambda system driven by a laser on the S-X transition. (c) Differential transmission dT/T (in color scale) on the T-X transition, with $\Omega_T = 1.0$ μeV; the contrast of the resonance is only -0.011%. Inset: Schematic energy diagram of the lambda system driven by a laser on the T-X transition.

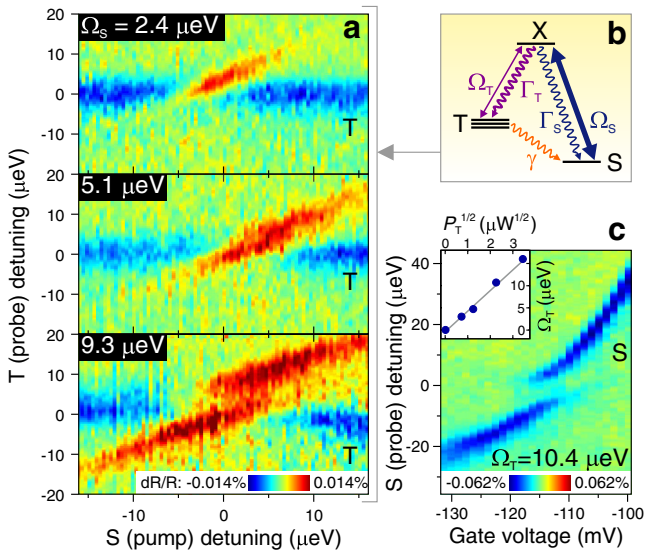

FIG. 4 (color online). (a) Differential reflection dR/R (in color scale) of a weak probe laser (Rabi frequency $\Omega_T = 0.6$ μeV) scanned across the T transition, in the presence of a strong but undetected pump laser stepped across the S transition, at $V = -94$ mV. The two lasers have orthogonal linear polarizations, allowing the reflected pump light to be extinguished by using a polarizer. The strong pump leads to small fluctuations in the exact resonance condition due to the creation of charges around the CQD [20]. The size of the Autler-Townes splitting in the bottom panel allows a calibration of Ω_S in terms of the pump laser power on the S transition, P_S. (b) Schematic energy level diagram of the lambda system formed by states S, T, and X. Ω_S and Ω_T indicate the laser Rabi frequencies; the effective spontaneous emission rate from X to the combined triplet states is about 3 times faster than to the singlet state ($\Gamma_T \approx 3\Gamma_S$). We observe fast relaxation (with rate γ) from T to S. (c) dR/R (in color scale) of a weak probe laser ($\Omega_S = 0.5$ μeV) scanned across the S transition, in the presence of a strong but undetected pump laser ($\Omega_T = 10.4$ μeV) resonant with the T transition, versus V. Inset: Ω_T as a function of the square root of the pump laser power $\sqrt{P_T}$. Ω_T is determined from the Rabi splitting in measurements as shown in the main panel.

from T to S. When the laser is tuned to the S resonance, relaxation counteracts optical shelving [23] in the T states and thus maintains the photon scattering rate (and therefore the dT or resonance fluorescence signal). In contrast, a laser on the T resonance quickly drives the system to the S state, where it remains shelved for a long time, since relaxation from S back to T is impeded by the 1.1 meV S-T energy difference. Thus, the overall photon scattering rate in this case is strongly reduced. Using a steady-state solution of the rate equations describing the S, T, and X populations [21], we can estimate the relaxation rate γ. The measured S:T scattering ratio of ~6–8 [obtained from the difference in dT contrast between Figs. 3(b) and 3(c) or from the difference in fluorescence intensity between the two traces in Fig. 3(a)] gives $\gamma/\Gamma \sim 0.1 - 0.25$, where $\Gamma = \Gamma_S + \Gamma_T \sim 1$ μeV is the total spontaneous emission rate from X.

The fast spin relaxation is most likely related to the large 1.1 meV exchange splitting between S and T states and the strong coupling to a degenerate electron gas in our device [24]. Both factors enhance the inelastic spin-flip cotunneling rate with the electron reservoir. Although fast spin relaxation is undesirable for using S and T_0 states to encode a qubit, it is essential for obtaining optical amplification, as we will now demonstrate.

We drive the system with a strong pump laser that is stepped across the S-X resonance and probe it by measuring the differential reflection (dR) of a weak probe laser scanned across the T-X resonance [25]. When the pump is far off resonance and has modest intensity [left and right sides of the top panel in Fig. 4(a)], the probe maps out the unperturbed T-X transition, similar to Fig. 3(c). As the pump gets closer to the S resonance (middle of the panel), the sign of the probe dR signal reverses, as indicated by the red color. This signifies that the probe laser actually *gains* intensity by interacting with the single CQD pair.

When the pump detuning is large (compared to the pump Rabi frequency Ω_S), the amplification can be considered as stemming from a stimulated Raman process [27]. Raman gain appears along the diagonal line in each panel in Fig. 4(a), where the two-photon resonance condition is fulfilled (detuning between the pump and probe laser equal to S-T splitting). In this limit, there is no significant population in the X state, and therefore no population inversion occurs between the bare X and T states [28]. In the opposite limit of small pump detuning and strong pump intensity, the nonperturbative coupling of the QD and the pump field leads to the formation of dressed states, which are coherent superpositions of states S and X [29]. Luminescence from these dressed states is predominantly incoherent, and optical amplification here results mainly from population inversion between the T state and either one of the dressed states. This is precisely what we observe in the Autler-Townes anticrossing that is seen in the lower panels of Fig. 4(a). To the best of our knowledge, this constitutes the first demonstration of optical amplification from dressed states observed in a lambda system.

As a control experiment, we tune the pump laser to the T transition and probe the S transition [Fig. 4(c)]. In this case, a standard (absorptive) Autler-Townes splitting is observed, without gain even for very high pump powers. This confirms that optical amplification on the S-X transition is prevented by the slow relaxation rate from S to T at low temperatures. This agrees with numerical simulations of the full 8-level system of S, T, and X states, which show qualitative agreement with the data [21].

In summary, we have demonstrated optical amplification in Raman transitions between singlet and triplet states of a single CQD molecule. This scheme is very promising for realizing a fully controllable solid-state single-emitter laser. In contrast to approaches based on the biexciton cascade [11] or p-state pumping [12] in single QDs, the CQD lambda system can be pumped fully coherently, and the depopulation rate between the optical ground states can be controlled by using the gate voltage or the tunnel barrier thickness. An alternative lambda scheme is provided by a one-electron QD in an in-plane magnetic field [30]. However, gain in such a system at 4 K would require a large field on the order of 10 T. In contrast, a CQD in the (1, 1) regime can provide gain even without a magnetic field. Moreover, the CQD can be tuned to opposite regimes: If it is sufficiently isolated from the electron reservoir (modest S-T splitting and a small cotunneling rate to the back contact), the lambda system enables ultrafast optical control of two-spin entanglement [16]. On the other hand, by designing a CQD molecule with a large S-T splitting and a strong cotunneling rate, the lambda system becomes ideal for generating laser amplification, even at elevated temperatures.

By coupling this new type of solid-state quantum emitter to a microcavity, it should be possible to observe laser oscillation. The photon statistics of such a laser are expected to differ from ordinary lasers. From the measured $\sim$0.014% single-pass gain, we estimate that a cavity quality factor of $\sim$7000 should enable laser oscillation. Using solid-immersion lenses to increase the gain could reduce the required Q factor by about an order of magnitude, making a practical implementation feasible.

We thank V. Golovach for discussions and C. Latta for help with the numerical simulations. This work is supported by the Swiss National Science Foundation NCCR Quantum Photonics project and an ERC Advanced Investigator grant (A. I.).

[1] Y. Mu and C. M. Savage, Phys. Rev. A **46**, 5944 (1992).
[2] P. R. Rice and H. J. Carmichael, Phys. Rev. A **50**, 4318 (1994).
[3] G. Björk, A. Karlsson, and Y. Yamamoto, Phys. Rev. A **50**, 1675 (1994).
[4] R. Jin *et al.*, Phys. Rev. A **49**, 4038 (1994).
[5] H.-J. Briegel, G. M. Meyer, and B.-G. Englert, Phys. Rev. A **53**, 1143 (1996).
[6] K. An *et al.*, Phys. Rev. Lett. **73**, 3375 (1994).
[7] J. McKeever *et al.*, Nature (London) **425**, 268 (2003).
[8] F. Dubin *et al.*, Nature Phys. **6**, 350 (2010).
[9] M. Nomura *et al.*, Nature Phys. **6**, 279 (2010).
[10] M. Winger *et al.*, Phys. Rev. Lett. **103**, 207403 (2009).
[11] I. A. Akimov, J. T. Andrews, and F. Henneberger, Phys. Rev. Lett. **96**, 067401 (2006).
[12] F. Sotier *et al.*, Nature Phys. **5**, 352 (2009).
[13] H. J. Krenner *et al.*, Phys. Rev. Lett. **94**, 057402 (2005).
[14] G. Ortner *et al.*, Phys. Rev. Lett. **94**, 157401 (2005).
[15] E. A. Stinaff *et al.*, Science **311**, 636 (2006).
[16] D. Kim *et al.*, Nature Phys. **7**, 223 (2010).
[17] M. F. Doty *et al.*, Phys. Rev. B **78**, 115316 (2008).
[18] R. Hanson *et al.*, Rev. Mod. Phys. **79**, 1217 (2007).
[19] R. J. Warburton *et al.*, Nature (London) **405**, 926 (2000).
[20] L. Robledo *et al.*, Science **320**, 772 (2008).
[21] See supplemental material at http://link.aps.org/supplemental/10.1103/PhysRevLett.107.017401 for additional information.
[22] A. N. Vamivakas *et al.*, Nature Phys. **5**, 198 (2009).
[23] M. Atatüre *et al.*, Science **312**, 551 (2006).
[24] Although the distance from the QD-B layer to the highly doped back contact was designed to be $\sim$50 nm, dopant segregation resulted in a much smaller effective distance, drastically increasing the spin-flip cotunneling rate. Experiments using CQDs with an S-T splitting of $\sim$100 μeV [16] did not exhibit fast relaxation; the observation of spin pumping in those experiments also indicates a weak coupling to the electron reservoir.
[25] The dR measurement detects the interference of the reflected probe laser with the CQD emission and is therefore sensitive only to *coherent* scattering [26].
[26] K. Karrai and R. J. Warburton, Superlattices Microstruct. **33**, 311 (2003).
[27] X. Xu *et al.*, Phys. Rev. Lett. **101**, 227401 (2008).
[28] M. O. Scully and M. S. Zubairy, *Quantum Optics* (Cambridge University Press, Cambridge, England, 1997).
[29] X. Xu *et al.*, Science **317**, 929 (2007).
[30] X. Xu *et al.*, Phys. Rev. Lett. **99**, 097401 (2007).